



Stellar spectroscopy in the near-infrared with a laser frequency comb

ANDREW J. METCALF,^{1,2} TYLER ANDERSON,³ CHAD F. BENDER,^{4,5} SCOTT BLAKESLEE,⁴ WESLEY BRAND,^{1,2} DAVID R. CARLSON,¹ WILLIAM D. COCHRAN,⁶ SCOTT A. DIDDAMS,^{1,2,15} MICHAEL ENDL,⁶ CONNOR FREDRICK,^{1,2} SAM HALVERSON,^{4,7} DANIEL D. HICKSTEIN,¹ FRED HEARTY,⁴ JEFF JENNINGS,^{1,2} SHUBHAM KANODIA,^{4,14} KYLE F. KAPLAN,⁵ ERIC LEVI,⁴ EMILY LUBAR,⁴ SUVRATH MAHADEVAN,^{4,14,16} ANDREW MONSON,⁴ JOE P. NINAN,^{4,14} COLIN NITROY,⁴ STEVE OSTERMAN,⁸ SCOTT B. PAPP,^{1,2} FRANKLYN QUINLAN,¹ LARRY RAMSEY,^{4,14} PAUL ROBERTSON,^{4,9} ARPITA ROY,^{4,10} CHRISTIAN SCHWAB,¹¹ STEINN SIGURDSSON,^{4,14} KARTIK SRINIVASAN,¹² GUDMUNDUR STEFANSSON,^{4,14} DAVID A. STERNER,⁴ RYAN TERRIEN,^{1,13} ALEX WOLSZCZAN,^{4,14} JASON T. WRIGHT,⁴ AND GABRIEL YCAS^{1,2}

¹Time and Frequency Division, National Institute of Standards and Technology, 325 Broadway, Boulder, Colorado 80305, USA

²Department of Physics, University of Colorado, 2000 Colorado Avenue, Boulder, Colorado 80309, USA

³Department of Physics, Pennsylvania State University, University Park, Pennsylvania 16802, USA

⁴Department of Astronomy & Astrophysics, Pennsylvania State University, 525 Davey Lab, University Park, Pennsylvania 16802, USA

⁵Steward Observatory, University of Arizona, Tucson, Arizona 85721, USA

⁶Department of Astronomy and McDonald Observatory, University of Texas at Austin, Austin, Texas 78712, USA

⁷MIT Kavli Institute for Astrophysics, 70 Vassar St, Cambridge, Massachusetts 02109, USA

⁸Johns Hopkins Applied Physics Lab, Laurel, Maryland 20723, USA

⁹Department of Physics and Astronomy, University of California-Irvine, Irvine, California 92697, USA

¹⁰California Institute of Technology, 1200 E California Blvd, Pasadena, California 91125, USA

¹¹Department of Physics and Astronomy, Macquarie University, Sydney, NSW 2109, Australia

¹²Microsystems and Nanotechnology Division, National Institute of Standards and Technology, 100 Bureau Drive, Gaithersburg, Maryland 20899, USA

¹³Department of Physics and Astronomy, Carleton College, Northfield, Minnesota 55057, USA

¹⁴Center for Exoplanets and Habitable Worlds, Pennsylvania State University, University Park, Pennsylvania 16802, USA

¹⁵e-mail: scott.diddams@nist.gov

¹⁶e-mail: suvrath@astro.psu.edu

Received 9 October 2018; revised 23 January 2019; accepted 28 January 2019 (Doc. ID 347824); published 20 February 2019

The discovery and characterization of exoplanets around nearby stars are driven by profound scientific questions about the uniqueness of Earth and our solar system, and the conditions under which life could exist elsewhere in our galaxy. Doppler spectroscopy, or the radial velocity (RV) technique, has been used extensively to identify hundreds of exoplanets, but with notable challenges in detecting terrestrial mass planets orbiting within habitable zones. We describe infrared RV spectroscopy at the 10 m Hobby–Eberly Telescope that leverages a 30 GHz electro-optic laser frequency comb with a nanophotonic supercontinuum to calibrate the Habitable Zone Planet Finder spectrograph. Demonstrated instrument precision <10 cm/s and stellar RVs approaching 1 m/s open the path to discovery and confirmation of habitable-zone planets around M -dwarfs, the most ubiquitous type of stars in our galaxy. © 2019

Optical Society of America under the terms of the [OSA Open Access Publishing Agreement](#)

<https://doi.org/10.1364/OPTICA.6.000233>

1. INTRODUCTION

Measurements of the periodic Doppler shift of a star using the spectroscopic radial velocity (RV) technique provide evidence of an unseen orbiting exoplanet and its minimum mass [1]. Complemented by photometric measurements of the transiting exoplanet [2], one can obtain the mass and radius (and density) of the exoplanet, which are critical parameters for classification and assessment of habitability. While the RV technique has been used extensively, the highest precision measurements have been limited to the visible region of the spectrum <700 nm,

and not the infrared [3]. Thus, 70% of the stars in our galaxy— M -dwarfs, which primarily emit in the near-infrared (NIR)—have largely been outside the efficient spectral grasp of the current generation of proven RV instruments [4]. Due to their proximity, abundance, and small radius and mass, M -dwarfs are very attractive targets in the search for habitable-zone rocky planets with NIR spectroscopy. The habitable zone [5] of an M -dwarf is close-in to the star, such that an orbiting Earth-mass planet within this zone induces an RV shift on the order of 1 m/s [6]. This is 10 times larger than the RV signature of Earth around the

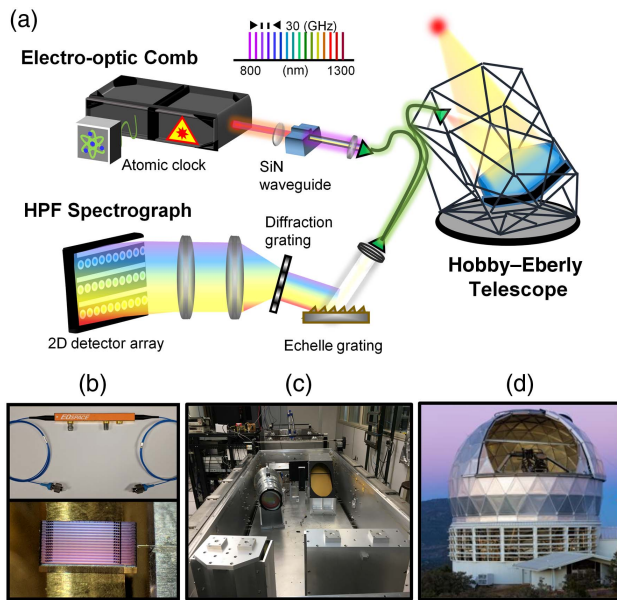


Fig. 1. Instrumentation for precision infrared astronomical RV spectroscopy. (a) Starlight is collected by the Hobby-Eberly telescope and directed to an optical fiber. Lasers, electro-optics, and nanophotonics are used to generate an optical frequency comb with teeth spaced by 30 GHz and stabilized to an atomic clock. Both the starlight and frequency comb light are coupled to the highly stabilized Habitable Zone Planet Finder (HPF) spectrograph where minute wavelength changes in the stellar spectrum are tracked with the precise calibration grid provided by the laser frequency comb. (b) Components for frequency comb generation: upper, a fiber-optic integrated electro-optic modulator; lower, silicon nitride chip (5 mm \times 3 mm) on which nano-photonic waveguides are patterned. Light is coupled into a waveguide from the left, and the supercontinuum is extracted from the right with a lensed fiber. (c) The HPF spectrograph, opened and showing the camera optics on the left, echelle grating on the right, and relay mirrors in front. The spectrograph footprint is approximately 1.5 m \times 3 m. (d) The 10 m Hobby-Eberly telescope at the McDonald Observatory in south-west Texas.

Sun, and significantly increases the detectability of such an Earth-mass planet. Stellar convection and magnetic activity (e.g., granulation and starspots) can obfuscate the small RV signature of terrestrial planets, but many of these noise sources are suppressed in the NIR compared to the optical [7]. High RV precision measurements of bright stars in the visible will benefit from complementary high RV precision NIR observations that better discriminate stellar activity from real planet signals [7,8].

While these motivations are well known, a combination of factors has limited the precision of even the best infrared RVs to 5–10 m/s over time scales of months [9,10]. Low-noise silicon detector arrays are not efficient at wavelengths beyond \sim 900 nm, requiring infrared detectors and cryogenic instruments. Existing wavelength calibration sources in the infrared are not yet as effective as iodine cells and thorium-argon lamps in the visible. Fiber-fed spectrographs with the required intrinsic stability in the infrared are only now being built and tested [11–13]. We overcome many technological and analysis hurdles that have impeded NIR RV measurements from reaching the \sim 1 m/s level, and we introduce a complete suite of infrared spectroscopic tools and techniques that provide the necessary precision for discovering and characterizing planetary systems around M-dwarf stars

(see Fig. 1). We have developed a 30 GHz optical frequency comb spanning 700–1600 nm built on integrated electro-optic (EO) modulators [14–16] and high-efficiency nanophotonic nonlinear waveguides [17,18] to provide a robust calibrator for long-term operation at the telescope. This comb-based calibrator provides tailored light to the stable Habitable Zone Planet Finder (HPF) spectrograph, designed and built from the ground up for precision infrared RVs [19]. The frequency comb and spectrograph have been installed at the 10 m Hobby-Eberly Telescope (HET), and we have demonstrated differential stellar RVs at 1.53 m/s (RMS) over months-long time scales, as well as shown that the comb-calibrated HPF can support RV precision as low as 6 cm/s.

To the best of our knowledge, this is the first time such RV precision has been realized in the NIR wavelength region beyond the spectral grasp of silicon detector arrays. This interdisciplinary result is an important step on the path to discovery and characterization of Earth-mass planets in the habitable zones of the nearest stars. The higher planet-to-star radius ratio in these M-dwarf systems will boost the transit signal by almost 2 orders of magnitude compared to Sun-like stars, making atmospheric studies of Earth-like planets feasible with current technology. Moreover, discovering and characterizing such targets is critical for the near-future detection of biomarkers in transiting terrestrial planetary atmospheres via spectroscopy with the James Webb Space Telescope [20].

2. FREQUENCY COMB INSTRUMENTATION

Optical frequency combs [21], which consist of an equally spaced array of laser frequencies, have been recognized as a critical component in precision astronomical RV measurements aimed at identifying Earth-like exoplanets [9,22–26]. However, the combination of spectral coverage across hundreds of nanometers, line spacing of many tens of GHz (needed for modern high-resolution astronomical spectrometers), operational robustness in an astronomical observatory environment, and high up-time requirements are challenging to achieve. Multiple frequency comb approaches targeting astronomical spectrograph calibration have been explored, including mode filtering [9,22–26], EO generation [15,27], and microresonators [28,29].

Our frequency comb is built around a combination of EO and integrated-photonics technologies to address the challenges of bandwidth, mode spacing, and robustness [see Fig. 2(a)]. In addition, we leverage recent advances with EO frequency combs to mitigate the impact of multiplicative microwave phase noise on the comb tooth linewidth and coherence [16,18]. The frequency comb begins with 1064 nm continuous wave (CW) light from a semiconductor laser that feeds waveguide EO modulators driven by a 30 GHz microwave source. This results in a comb of approximately 100 teeth spaced exactly by the microwave drive frequency. The CW laser, microwave source, and all other frequencies in the system are referenced to a GPS-disciplined clock that provides absolute traceability to the SI second. The initial comb is next passed through a 30 GHz Fabry-Perot cavity that acts to filter and reduce the impact of broad bandwidth electronic thermal noise [16]. The frequency comb is then amplified in an ytterbium fiber amplifier, spectrally broadened and temporally compressed to a pulse width of 70 fs, and finally focused into a 25 mm long nonlinear silicon nitride (SiN)

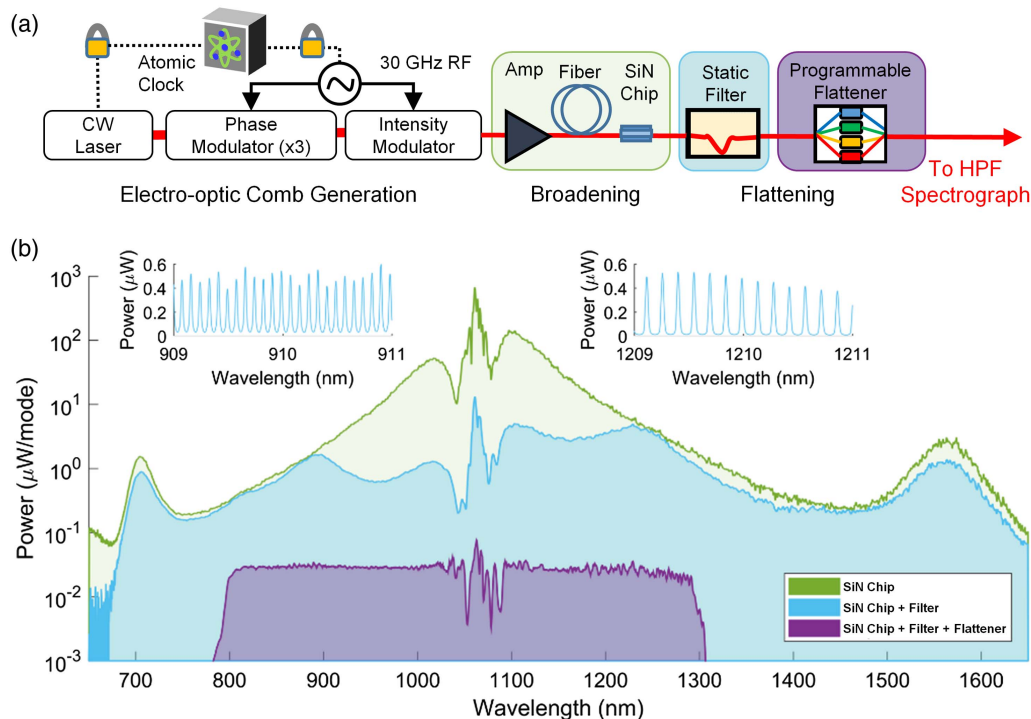


Fig. 2. 30 GHz electro-optic frequency comb. (a) The frequency comb is generated via electro-optic modulation of a continuous wave (CW) laser followed by nonlinear spectral broadening and amplitude filtering stages to tailor the spectrum. (b) The spectral envelopes recorded with a low-resolution grating spectrometer at different points in the setup: green, at the output of the SiN chip waveguide; blue, after a static amplitude filter; purple, after a programmable amplitude filter. The two insets are high-resolution recordings of the 30 GHz comb modes centered at 910 and 1210 nm, respectively.

waveguide [17,18]. The experimental setup is covered in more detail in Supplement 1.

The waveguide is 750 nm wide and 690 nm thick, which provides the combination of tight confinement and engineered dispersion to achieve a supercontinuum spectrum spanning 700–1600 nm with only 525 mW of incident average power (18 pJ of pulse energy). This low power reduces the thermal loading and aids the long-term operability. Following spectral generation, a combination of static and programmable amplitude filters [30] is used to tailor the spectral envelope. The output of each amplitude filtering stage is shown in Fig. 2(b) along with high-resolution insets that show the resolved 30 GHz comb modes at 910 and 1210 nm. Optical heterodyne measurements between the 30 GHz comb and a frequency-stabilized reference laser confirm that the stability of the comb matches that of the GPS-disciplined clock with fractional uncertainty of 2×10^{-11} at 1 s, and $<3 \times 10^{-13}$ for time scales of one day and longer. Significantly, EO frequency combs could be employed for coverage from <600 nm to >2500 nm [17,18].

The entire frequency comb has been assembled on a 60 cm \times 152 cm breadboard and installed at the HET at McDonald Observatory, together with the HPF spectrograph. The HPF is a vacuum-housed cross-dispersed echelle spectrograph with dimensions of approximately 1.5 m \times 3 m and resolving power of $R = \lambda/\Delta\lambda \sim 53,000$. The spectrograph is designed and optimized for stability, with its optics platform cryogenically cooled and temperature stabilized at the milliKelvin level [19,31]. The 28 echelle orders cover the wavelength range 810–1280 nm, and the spectra are recorded on a 2048 \times 2048 pixel Hawaii-2 (H2RG) mercury–cadmium–telluride (HgCdTe) infrared

detector array that has a 1.7 μm long wavelength cutoff. The HPF entrance slit is fed by three optical fibers that can be simultaneously illuminated with star, sky, and calibration light to track the instrument drift. A more detailed description of experimental methods is provided in Supplement 1.

3. SPECTROGRAPH CALIBRATION AND RADIAL VELOCITY MEASUREMENTS

The frequency comb was integrated into the HPF calibration system at the end of February 2018 and has been operating continuously and autonomously since early May 2018. The light from the comb system is coupled to the HPF calibration source-selector system (see Kanodia *et al.* [32] for a layout) with a 50 μm diameter multimode fiber. This selector couples the light from any source (including the comb) into a 300 μm dynamic fiber agitator, which is coupled to one part of a 2 inch integrating sphere. We have shown [33] that the combination of temporal scrambling and an integrating sphere is effective at minimizing modal noise to deliver a constant illumination. The dynamic fiber agitator is a customizable commercial system from Giga Concept that applies torsional oscillations to the fiber (under compression) at a few Hz. An identical second fiber agitator is also used to couple the calibration light to the calibration fiber coupled to the telescope facility calibration unit.

On-sky stellar observations of stable M -dwarfs and stars with known orbiting planets have been employed to characterize the system's present RV precision. Figure 3(a) shows example stellar and comb spectra as recorded on the HgCdTe array, illustrating the HPF's spectral range and the uniformity of the comb across

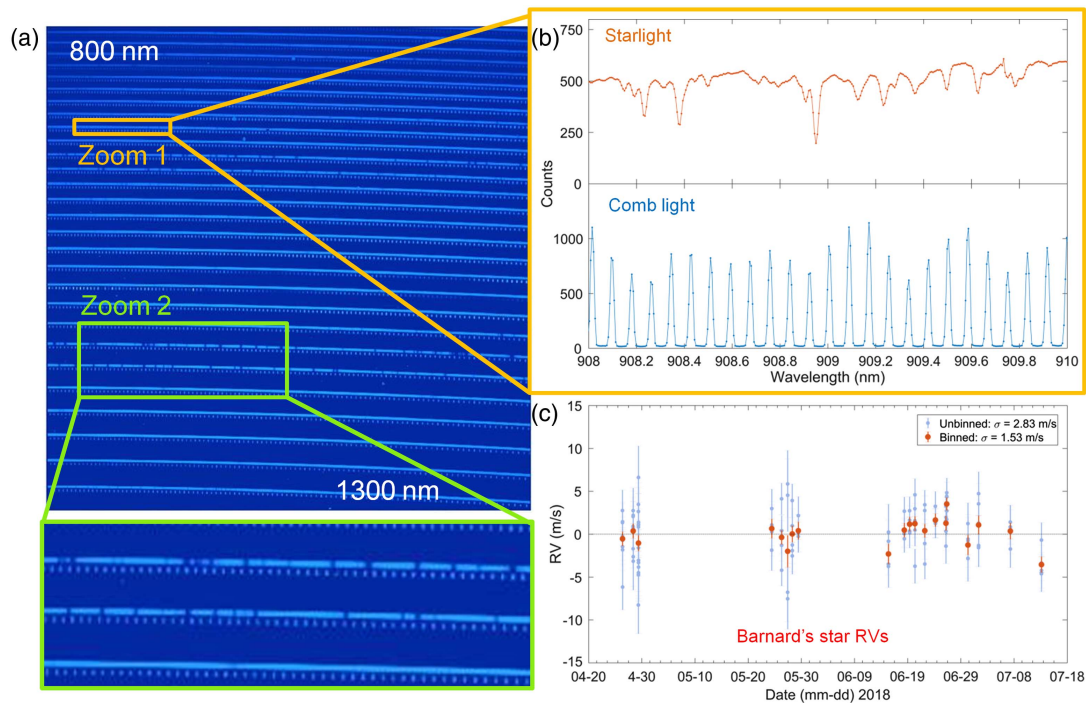


Fig. 3. On-sky data taken at the Hobby–Eberly telescope using the HPF spectrograph and laser frequency comb as a real-time calibrator. (a) Echellogram from the HPF detector array when illuminated by both the frequency comb and starlight from the telescope. The left image shows the full detector readout of the 28 echelle orders spanning 810–1280 nm. “Zoom 2” shows a smaller region where the vertical offset between the wavelength-matched star and comb light can be visualized. (b) “Zoom 1” shows the extracted stellar spectrum and comb calibration around 909 nm. (c) Three months of precision on-sky RV data of Barnard’s star. Unbinned observations (5 min cadence) are shown in blue. The binned observations are shown in red. The red points all have an equivalent on-sky exposure time of 20 min or greater (see Table S1 in Supplement 1 for the binned RVs along with a listing of equivalent exposure times).

the 28 orders. Using the comb as a reference, a wavelength solution is derived for each order that is subsequently used to calibrate the corresponding stellar spectra. Benchmarking the full instrumental chain (from telescope to comb to detector), as well as spectral extraction, RV measurement algorithms, and corrections of barycentric RV, require on-sky observations of a star that is intrinsically stable or has a known RV signal. Barnard’s star is a bright nearby star of spectral type $\sim M4$. While its RVs show a low-amplitude signal attributed to an exoplanet [34], it is still among the most stable M stars known. Figure 3(b) shows the residual RVs of Barnard’s star from 118 high signal-to-noise measurements over a three-month period. Observations were limited to 5 min exposures to prevent saturation of the NIR detector. The scatter of individual (5 min) RV measurements is 2.83 m/s, and when data within a ~ 1 -h HET observation window (or track) are binned to increase the signal to noise, the scatter is reduced to 1.53 m/s. This RV precision is unprecedented in the NIR, and approaches that of the best measurements for this star with visible-band spectrometers (e.g., 1.23 m/s using the HARPS instrument [35]). A more detailed description of experimental methods is provided in Supplement 1.

Additional experiments allow us to probe the intrinsic calibration stability of the HPF spectrograph independent of stellar observations. To accomplish this, we take advantage of an auxiliary optical fiber that transmits the laser comb light to the primary focus of the telescope, where it is diffused and sent to the HPF spectrograph through both the “science” and “sky” fibers (Fig. 4(a)). In this arrangement, two sets of comb calibration

spectra are recorded by HPF and processed to provide RV wavelength solutions from both fiber channels. As the stable frequency comb is common to the fibers, the retrieved RVs will reveal the slow drift of the HPF in each channel. However, the difference of the two channels should ideally be zero within the uncertainty of the photon noise. As such, this measurement allows us to carefully probe noncommon-mode variations between the light paths from the two fibers to the detector array that would ultimately limit the RV precision. Such instabilities could arise from independent drifts in the optical fiber feeds, the spectrograph optics, systematics and noise in the HgCdTe detector array, or data reduction issues.

Measurements were taken over multiple nights, and the absolute drift of the HPF is recorded in both channels every 5 or 10 min, with the results shown in Fig. 4(b). As seen in these data, the drift of the HPF was about 5–7 m/s during a 5–10 h measurement window, with larger daily excursions due to the liquid nitrogen fills. The difference of the RVs of the two channels is shown in Fig. 4(c), revealing that the scatter of a single 10 min differential drift measurement is at the 20 cm/s level. We further see that if we bin multiple measurements, the RV precision improves approximately as the square root of total measurement time to as low as 6 cm/s at 300 min [Fig. 4(d)]. Furthermore, we observe no statistically significant drift in the difference of the RVs retrieved from the two fibers over six days.

These data support the assertion that the comb-calibrated HPF has the intrinsic stability to support infrared spectroscopy with precision below 10 cm/s. With the HET, this was a

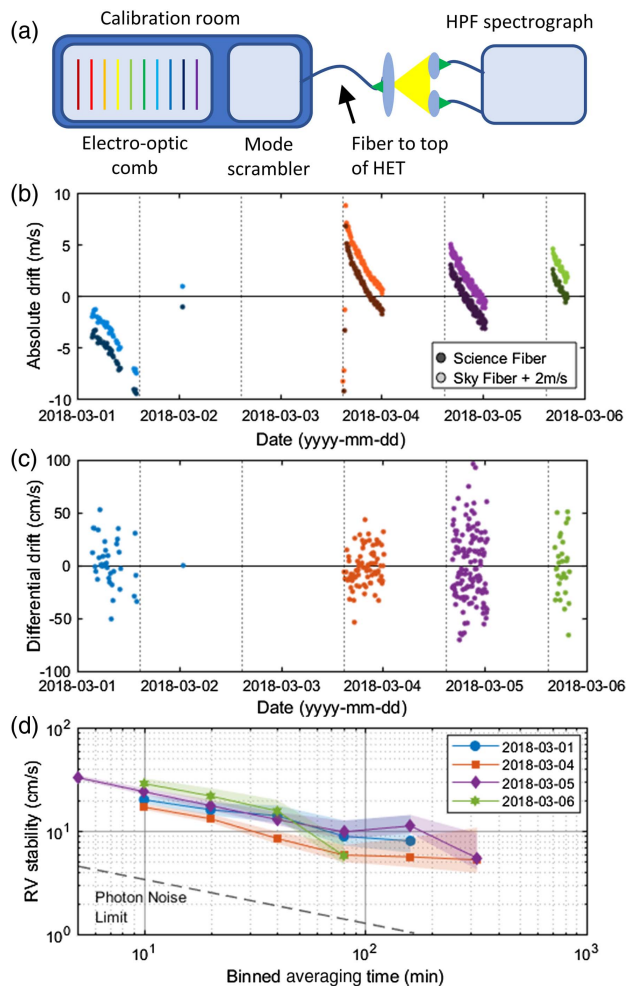


Fig. 4. Characterization of the radial velocity measurement precision of the HPF spectrograph. (a) Experimental setup. The laser frequency comb light is coupled via the HPF calibration bench and a fiber scrambler into an auxiliary optical fiber whose output is diffused across the HET focal plane to illuminate the HPF “science” and “sky” fibers. These fibers carry the light to the HPF spectrograph, where it is dispersed and detected on the HgCdTe detector array. (b) Absolute drifts of the HPF measured in the two fiber channels over four nights of tests. Each point is a 10 min exposure, except for data on 03–05, where the exposure time is 5 min. Note, the RVs from the “science” fiber are offset by 2 m/s in the plot for clarity. The total daily peak-to-peak drift of HPF is 15–20 m/s, which is primarily caused by daily liquid nitrogen fills. Dashed lines show the time of these daily fills. The HPF was also exponentially approaching thermal stability in March when this test was performed. (c) The difference of the drifts between the RVs recovered from the “sky” and the “science” fibers. (d) Characterization of the RV stability by successive binning of measurements. This demonstrates that binning to effective averaging time of 300 min results in RV stability below 10 cm/s.

particularly harsh test since the calibration light splays across a significant fraction of the 30 arcmin focal plane—leading to fiber modal noise, which is known to be worse in the NIR than the optical. A fiber-based mode scrambler was used to mitigate modal noise, but it likely does not fully solve this issue. Our measured RV scatter is currently about 5 times greater than the photon-limited precision (3.7 cm/s in 10 min). Further improvements towards the photon-limited precision should be possible with

algorithmic improvements, better characterization of the NIR detectors, and better modal scrambling.

4. DISCUSSION AND CONCLUSION

In summary, we have introduced a new frequency comb platform in the NIR (700–1600 nm) that leverages the reliability of telecom EO modulators and efficient chip-integrated nonlinear waveguides to provide an ultrastable calibrator for the HPF spectrograph. Since May 2018, the frequency comb and HPF instruments have been running autonomously at the 10 m HET, enabling high-cadence RV measurements on one of the largest optical telescopes in the world. This combination of instrumentation forms a unique and powerful set of tools for exoplanet science focused on M-dwarfs. Our stellar RV measurements with scatter of 1.53 m/s are presently the most precise achieved in the NIR with HgCdTe detector arrays, and now approach the best RV measurements with more mature visible wavelength silicon detectors and associated technology, to the best of our knowledge. Within this context, the instrumentation and techniques we introduce represent a significant step towards the long-desired goal of RV spectroscopy in the NIR with precision at (and below) 1 m/s, as will be critical for the discovery and characterization of Earth-mass planets in the habitable zones of the nearest stars.

Finally, during the review of this paper, Ribas *et al.* [34] announced the discovery of a 3.2 Earth-mass (RV amplitude = 1.2 m/s) exoplanet candidate orbiting Barnard’s star with a period of 233 days. While our HPF RVs are not inconsistent with the orbit proposed by Ribas *et al.*, our observations extending over 86 days coincided with the least dynamic region of the orbital phase curve, resulting in the flat time series shown in Fig. 3(c). Nonetheless, it is significant that our first RVs from the comb-calibrated HPF are at a level of precision that makes them relevant for state-of-the-art exoplanet astrophysics. Further discussion of our RVs in the context of this exoplanet candidate is found in Supplement 1.

Funding. National Science Foundation (NSF) (AST-100667, AST-1126413, AST-1310875, AST-1310885); National Institute of Standards and Technology (NIST) (On-a-Chip Program); National Aeronautics and Space Administration (NASA) (NNX09AB34G); Pennsylvania State University and its Center for Exoplanets and Habitable Worlds; National Aeronautics and Space Administration (NASA) (NNX16A028H, Sagan Fellowship); Heising-Simons Foundation (2017-0494).

Acknowledgment. We thank the three anonymous reviewers for comments and suggestions that have improved the quality of this work. We thank Zach Newman for his comments on this manuscript and Ian Coddington for his contributions to the development of the laser frequency comb. We thank the HET staff for their critical assistance, expertise, and support. This work would not be possible without them. We are very grateful for help and support from Gary Hill, Hansin Lee, Brian Vattiat, and Phillip McQueen. Data presented herein were obtained at the HET, a joint project of the University of Texas at Austin, the Pennsylvania State University, Ludwig-Maximilians-Universität München, and Georg-August Universität Göttingen. The HET is named in honor of its principal benefactors, William P. Hobby and Robert E. Eberly. The HET collaboration acknowledges the

support and resources from the Texas Advanced Computing Center. Computations for this research were performed on the Pennsylvania State University's Institute for CyberScience Advanced CyberInfrastructure (ICS-ACI).

See Supplement 1 for supporting content.

REFERENCES

- M. Mayor and D. Queloz, "A Jupiter-mass companion to a solar-type star," *Nature* **378**, 355–359 (1995).
- J. N. Winn, "Exoplanet transits and occultations," in *Exoplanets*, S. Seager, ed. (University of Arizona, 2011), pp. 55–77.
- D. A. Fischer, G. Anglada-Escude, P. Arriagada, R. V. Baluev, J. L. Bean, F. Bouchy, L. A. Buchhave, T. Carroll, A. Chakraborty, J. R. Crepp, R. I. Dawson, S. A. Diddams, X. Dumusque, J. D. Eastman, M. Endl, P. Figueira, E. B. Ford, D. Foreman-Mackey, P. Fournier, G. Fűrész, B. S. Gaudi, P. C. Gregory, F. Grundahl, A. P. Hatzes, G. Hébrard, E. Herrero, D. W. Hogg, A. W. Howard, J. A. Johnson, P. Jorden, C. A. Jurgenson, D. W. Latham, G. Laughlin, T. J. Loredo, C. Lovis, S. Mahadevan, T. M. McCracken, F. Pepe, M. Perez, D. F. Phillips, P. P. Plavchan, L. Prato, A. Quirrenbach, A. Reiners, P. Robertson, N. C. Santos, D. Sawyer, D. Segransan, A. Sozzetti, T. Steinmetz, A. Szentgyorgyi, S. Udry, J. A. Valenti, S. X. Wang, R. A. Wittenmyer, and J. T. Wright, "State of the field: extreme precision radial velocities," *Publ. Astron. Soc. Pac.* **128**, 066001 (2016).
- T. J. Henry, W.-C. Jao, J. P. Subasavage, T. D. Beaulieu, P. A. Ianna, E. Costa, and R. A. Mendez, "The solar neighborhood. XVII. Parallax results from the CTIOPI 0.9 m program: 20 new members of the RECONS 10 parsec sample," *Astron. J.* **132**, 2360–2371 (2006).
- R. K. Kopparapu, R. Ramirez, J. F. Kasting, V. Eymet, T. D. Robinson, S. Mahadevan, R. C. Terrien, S. Domagal-Goldman, V. Meadows, and R. Deshpande, "Habitable zones around main-sequence stars: new estimates," *Astrophys. J.* **765**, 131 (2013).
- G. Anglada-Escude, P. J. Amado, J. Barnes, Z. M. Berdiñas, R. P. Butler, G. A. L. Coleman, I. de la Cueva, S. Dreizler, M. Endl, B. Giesers, S. V. Jeffers, J. S. Jenkins, H. R. A. Jones, M. Kiraga, M. Kürster, M. J. López-González, C. J. Marvin, N. Morales, J. Morin, R. P. Nelson, J. L. Ortiz, A. Ofir, S.-J. Paardekooper, A. Reiners, E. Rodríguez, C. Rodríguez-López, L. F. Sarmiento, J. P. Strachan, Y. Tsapras, M. Tuomi, and M. Zechmeister, "A terrestrial planet candidate in a temperate orbit around Proxima Centauri," *Nature* **536**, 437–440 (2016).
- R. C. Marchwinski, S. Mahadevan, P. Robertson, L. Ramsey, and J. Harder, "Toward understanding stellar radial velocity jitter as a function of wavelength: the sun as a proxy," *Astrophys. J.* **798**, 63 (2015).
- P. Robertson, S. Mahadevan, M. Endl, and A. Roy, "Stellar activity masquerading as planets in the habitable zone of the M dwarf Gliese 581," *Science* **345**, 440–444 (2014).
- G. G. Ycas, F. Quinlan, S. A. Diddams, S. Osterman, C. Bender, B. Botzer, L. Ramsey, R. Terrien, S. Mahadevan, and S. Redman, "Demonstration of on-sky calibration of astronomical spectra using a 25 GHz near-IR laser frequency comb," *Opt. Express* **20**, 6631–6643 (2012).
- J. Bean, A. Seifahrt, H. Hartman, H. Nilsson, G. Wiedemann, A. Reiners, S. Dreizler, and T. Henry, "The CRIRES search for planets around the lowest-mass stars. I. High-precision near-infrared radial velocities with an ammonia gas cell," *Astrophys. J.* **713**, 410–422 (2009).
- A. Quirrenbach, P. J. Amado, J. A. Caballero, R. Mundt, A. Reiners, I. Ribas, W. Seifert, M. Abril, J. Aceituno, F. J. Alonso-Floriano, H. Anwand-Heerwart, M. Azzaro, F. Bauer, D. Barrado, S. Becerril, V. J. S. Bejar, D. Benitez, Z. M. Berdinas, M. Brinkmüller, M. C. Cardenas, E. Casal, A. Claret, J. Colomé, M. Cortes-Contreras, S. Czesla, M. Doellinger, S. Dreizler, C. Feiz, M. Fernandez, I. M. Ferro, B. Fuhrmeister, D. Galadi, I. Gallardo, M. C. Gálvez-Ortiz, A. Garcia-Piquer, R. Garrido, L. Gesa, V. Gómez Galera, J. I. González Hernández, R. Gonzalez Peinado, U. Grözinger, J. Guàrdia, E. W. Guenther, E. de Guindos, H.-J. Hagen, A. P. Hatzes, P. H. Hauschildt, J. Helmling, T. Henning, D. Hermann, R. Hernández Arabi, L. Hernández Castaño, F. Hernández Hernando, E. Herrero, A. Huber, K. F. Huber, P. Huke, S. V. Jeffers, E. de Juan, A. Kaminski, M. Kehr, M. Kim, R. Klein, J. Klüter, M. Kürster, M. Lafarga, L. M. Lara, A. Lamert, W. Laun, R. Launhardt, U. Lemke, R. Lenzen, M. Llamas, M. Lopez del Fresno, M. López-Puertas, J. López-Santiago, J. F. Lopez Salas, H. Magan Madinabeitia, U. Mall, H. Mandel, L. Mancini, J. A. Marin Molina, D. Maroto Fernández, E. L. Martín, S. Martín-Ruiz, C. Marvin, R. J. Mathar, E. Mirabet, D. Montes, J. C. Morales, R. Morales Muñoz, E. Nagel, V. Naranjo, G. Nowak, E. Palle, J. Panduro, V. M. Passegger, A. Pavlov, S. Pedraz, E. Perez, D. Pérez-Medialdea, M. Perger, M. Pluto, A. Ramón, R. Rebolo, P. Redondo, S. Reffert, S. Reinhard, P. Rhode, H.-W. Rix, F. Rodler, E. Rodríguez, C. Rodríguez López, R. R. Rohloff, A. Rosich, M. A. Sanchez Carrasco, J. Sanz-Forcada, P. Sarkis, L. F. Sarmiento, S. Schäfer, J. Schiller, C. Schmidt, J. H. M. M. Schmitt, P. Schöfer, A. Schweitzer, D. Shulyak, E. Solano, O. Stahl, C. Storz, H. M. Tabernero, M. Tala, L. Tal-Or, R.-G. Ulbrich, G. Veredas, J. I. Vico Linares, F. Vilardell, K. Wagner, J. Winkler, M.-R. Zapatero Osorio, M. Zechmeister, M. Ammler-von Eiff, G. Anglada-Escudé, C. del Burgo, M. L. Garcia-Vargas, A. Klutsch, J.-L. Lizon, M. Lopez-Morales, A. Ofir, A. Pérez-Calpena, M. A. C. Perryman, E. Sánchez-Blanco, J. B. P. Strachan, J. Stürmer, J. C. Suárez, T. Trifonov, S. M. Tulloch, and W. Xu, "CARMENES: an overview six months after first light," *Proc. SPIE* **9908**, 990814 (2016).
- É. Artigau, D. Kouach, J.-F. Donati, R. Doyon, X. Delfosse, S. Baratchart, M. Lacombe, C. Moutou, P. Rabou, L. P. Parès, Y. Micheau, S. Thibault, V. A. Reshetov, B. Dubois, O. Hernandez, P. Vallée, S.-Y. Wang, F. Dolon, F. A. Pepe, F. Bouchy, N. Striebig, F. Hénault, D. Loop, L. Saddlemyer, G. Barrick, T. Vermeulen, M. Dupieux, G. Hébrard, I. Boisse, E. Martioli, S. H. P. Alencar, J.-D. do Nascimento, and P. Figueira, "SPIRou: the near-infrared spectropolarimeter/high-precision velocimeter for the Canada-France-Hawaii telescope," *Proc. SPIE* **9147**, 914713 (2014).
- T. Kotani, M. Tamura, H. Suto, J. Nishikawa, B. Sato, W. Aoki, T. Usuda, T. Kurokawa, K. Kashiwagi, S. Nishiyama, Y. Ikeda, D. B. Hall, K. W. Hodapp, J. Hashimoto, J.-I. Morino, Y. Okuyama, Y. Tanaka, S. Suzuki, S. Inoue, J. Kwon, T. Suenaga, D. Oh, H. Baba, N. Narita, E. Kokubo, Y. Hayano, H. Izumiura, E. Kambe, T. Kudo, N. Kusakabe, M. Ikoma, Y. Hori, M. Omiya, H. Genda, A. Fukui, Y. Fujii, O. Guyon, H. Harakawa, M. Hayashi, M. Hidaï, T. Hirano, M. Kuzuhara, M. Machida, T. Matsuo, T. Nagata, H. Onuki, M. Ogihara, H. Takami, N. Takato, Y. H. Takahashi, C. Tachinami, H. Terada, H. Kawahara, and T. Yamamuro, "Infrared Doppler instrument (IRD) for the Subaru telescope to search for Earth-like planets around nearby M-dwarfs," *Proc. SPIE* **9147**, 914712 (2014).
- A. J. Metcalf, V. Torres-Company, D. E. Leaird, and A. M. Weiner, "High-power broadly tunable electrooptic frequency comb generator," *IEEE J. Sel. Top. Quantum Electron.* **19**, 231–236 (2013).
- X. Yi, K. Vahala, J. Li, S. Diddams, G. Ycas, P. Plavchan, S. Leifer, J. Sandhu, G. Vasisht, P. Chen, P. Gao, J. Gagne, E. Furlan, M. Bottom, E. C. Martin, M. P. Fitzgerald, G. Doppmann, and C. Beichman, "Demonstration of a near-IR line-referenced electro-optical laser frequency comb for precision radial velocity measurements in astronomy," *Nat. Commun.* **7**, 10436 (2016).
- K. Beha, D. C. Cole, P. Del'Haye, A. Coillet, S. A. Diddams, and S. B. Papp, "Electronic synthesis of light," *Optica* **4**, 406–411 (2017).
- D. R. Carlson, D. D. Hickstein, A. Lind, J. B. Olson, R. W. Fox, R. C. Brown, A. D. Ludlow, Q. Li, D. Westly, H. Leopardi, T. M. Fortier, K. Srinivasan, S. A. Diddams, and S. B. Papp, "Photonic-chip supercontinuum with tailored spectra for precision frequency metrology," *Phys. Rev. Appl.* **8**, 014027 (2017).
- D. R. Carlson, D. D. Hickstein, W. Zhang, A. J. Metcalf, F. Quinlan, S. A. Diddams, and S. B. Papp, "Ultrafast electro-optic light with subcycle control," *Science* **361**, 1358–1363 (2018).
- S. Mahadevan, L. W. Ramsey, R. Terrien, S. Halverson, A. Roy, F. Hearty, E. Levi, G. K. Stefansson, P. Robertson, C. Bender, C. Schwab, and M. Nelson, "The habitable-zone planet finder: a status update on the development of a stabilized fiber-fed near-infrared spectrograph for the Hobby-Eberly telescope," *Proc. SPIE* **9147**, 914710 (2014).
- S. Seager, W. Bains, and R. Hu, "Biosignature Gases in H₂-dominated Atmospheres on Rocky Exoplanets," *Astrophys. J.* **777**, 95 (2013).
- S. A. Diddams, "The evolving optical frequency comb," *J. Opt. Soc. Am. B* **27**, B51–B62 (2010).
- M. T. Murphy, T. Udem, R. Holzwarth, A. Sizmann, L. Pasquini, C. Araujo-Hauck, H. Dekker, S. D'Odorico, M. Fischer, T. W. Hänsch,

- and A. Manescau, "High-precision wavelength calibration of astronomical spectrographs with laser frequency combs," *Mon. Not. R. Astron. Soc.* **380**, 839–847 (2007).
23. D. Braje, M. Kirchner, S. Osterman, T. Fortier, and S. A. Diddams, "Astronomical spectrograph calibration with broad-spectrum frequency combs," *Eur. Phys. J. D* **48**, 57–66 (2008).
 24. C.-H. Li, A. J. Benedick, P. Fendel, A. G. Glenday, F. X. Kartner, D. F. Phillips, D. Sasselov, A. Szentgyorgyi, and R. L. Walsworth, "A laser frequency comb that enables radial velocity measurements with a precision of 1 cm s^{-1} ," *Nature* **452**, 610–612 (2008).
 25. T. Steinmetz, T. Wilken, C. Araujo-Hauck, R. Holzwarth, T. W. Hänsch, L. Pasquini, A. Manescau, S. D'Odorico, M. T. Murphy, T. Kentischer, W. Schmidt, and T. Udem, "Laser frequency combs for astronomical observations," *Science* **321**, 1335–1337 (2008).
 26. T. Wilken, G. Lo Curto, R. A. Probst, T. Steinmetz, A. Manescau, L. Pasquini, J. I. Gonzalez Hernandez, R. Rebolo, T. W. Hänsch, T. Udem, and R. Holzwarth, "A spectrograph for exoplanet observations calibrated at the centimetre-per-second level," *Nature* **485**, 611–614 (2012).
 27. E. Obrzud, M. Rainer, A. Harutyunyan, B. Chazelas, M. Ceconi, A. Ghedina, E. Molinari, S. Kundermann, S. Lecomte, F. Pepe, F. Wildi, F. Bouchy, and T. Herr, "Broadband near-infrared astronomical spectrometer calibration and on-sky validation with an electro-optic laser frequency comb," arXiv:1808.00860v2 (2018).
 28. E. Obrzud, M. Rainer, A. Harutyunyan, M. H. Anderson, M. Geiselman, B. Chazelas, S. Kundermann, S. Lecomte, M. Ceconi, A. Ghedina, E. Molinari, F. Pepe, F. Wildi, F. Bouchy, T. J. Kippenberg, and T. Herr, "A microphotonic astrocomb," *Nat. Photon.* **13**, 31–35 (2019).
 29. M.-G. Suh, X. Yi, Y.-H. Lai, S. Leifer, I. S. Grudin, G. Vasisht, E. C. Martin, M. P. Fitzgerald, G. Doppmann, J. Wang, D. Mawet, S. B. Papp, S. A. Diddams, C. Beichman, and K. Vahala, "Searching for exoplanets using a microresonator astrocomb," *Nat. Photon.* **13**, 25–30 (2019).
 30. A. M. Weiner, "Ultrafast optical pulse shaping: a tutorial review," *Opt. Commun.* **284**, 3669–3692 (2011).
 31. G. K. Stefansson, F. R. Hearty, P. M. Robertson, S. Mahadevan, T. B. Anderson, E. I. Levi, C. F. Bender, M. J. Nelson, A. J. Monson, B. Blank, S. P. Halverson, C. Henderson, L. W. Ramsey, A. Roy, C. Schwab, and R. C. Terrien, "A versatile technique to enable sub-milli-Kelvin instrument stability for precise radial velocity measurements: tests with the Habitable-zone Planet Finder," *Astrophys. J.* **833**, 175 (2016).
 32. S. Kanodia, S. Mahadevan, L. Ramsey, G. Stefansson, A. Monson, F. Hearty, S. Blakeslee, E. Lubar, C. Bender, J. Ninan, D. Sterner, A. Roy, S. P. Halverson, and P. Robertson, "Overview of the spectrometer optical fiber feed for the habitable-zone planet finder," *Proc. SPIE* **10702**, 107026Q (2018).
 33. S. Mahadevan, S. Halverson, L. Ramsey, and N. Venditti, "Suppression of fiber modal noise induced radial velocity errors for bright emission-line calibration sources," *Astrophys. J.* **786**, 18 (2014).
 34. I. Ribas, M. Tuomi, A. Reiners, R. P. Butler, J. C. Morales, M. Perger, S. Dreizler, C. Rodríguez-López, J. I. González Hernández, A. Rosich, F. Feng, T. Trifonov, S. S. Vogt, J. A. Caballero, A. Hatzes, E. Herrero, S. V. Jeffers, M. Lafarga, F. Murgas, R. P. Nelson, E. Rodríguez, J. B. P. Strachan, L. Tal-Or, J. Teske, B. Toledo-Padrón, M. Zechmeister, A. Quirrenbach, P. J. Amado, M. Azzaro, V. J. S. Béjar, J. R. Barnes, Z. M. Berdiñas, J. Burt, G. Coleman, M. Cortés-Contreras, J. Crane, S. G. Engle, E. F. Guinan, C. A. Haswell, T. Henning, B. Holden, J. Jenkins, H. R. A. Jones, A. Kaminski, M. Kiraga, M. Kürster, M. H. Lee, M. J. López-González, D. Montes, J. Morin, A. Ofir, E. Pallé, R. Rebolo, S. Reffert, A. Schweitzer, W. Seifert, S. A. Shectman, D. Staab, R. A. Street, A. Suárez Mascareño, Y. Tsapras, S. X. Wang, and G. Anglada-Escudé, "A candidate super-Earth planet orbiting near the snow line of Barnard's star," *Nature* **563**, 365–368 (2018).
 35. G. Anglada-Escudé and R. P. Butler, "The HARPS-TERRA project. I. Description of the algorithms, performance, and new measurements on a few remarkable stars observed by HARPS," *Astrophys. J. Suppl. Ser.* **200**, 15 (2012).